

Video Article

Bioprintable Alginate/Gelatin Hydrogel 3D *In Vitro* Model Systems Induce Cell Spheroid Formation

Tao Jiang¹, Jose Munguia-Lopez^{2,3}, Salvador Flores-Torres², Joel Grant⁴, Sanahan Vijayakumar⁴, Antonio De Leon-Rodriguez³, Joseph M. Kinsella^{2,5}

¹Department of Mechanical Engineering, McGill University Montreal

²Department of Bioengineering, McGill University Montreal

³Department of Molecular Biology, Instituto Potosino de Investigación Científica y Tecnológica, A.C. (IPICYT)

⁴Department of Mining and Materials Engineering, McGill University Montreal

⁵Department of Biomedical Engineering, McGill University Montreal

*These authors contributed equally

Correspondence to: Joseph M. Kinsella at joseph.kinsella@mcgill.ca

URL: <https://www.jove.com/video/57826>

DOI: [doi:10.3791/57826](https://doi.org/10.3791/57826)

Keywords: Bioengineering, Issue 137, 3D bioprinting, hydrogel, cancer cells, tumor spheroids, alginate, gelatin

Date Published: 7/2/2018

Citation: Jiang, T., Munguia-Lopez, J., Flores-Torres, S., Grant, J., Vijayakumar, S., De Leon-Rodriguez, A., Kinsella, J.M. Bioprintable Alginate/Gelatin Hydrogel 3D *In Vitro* Model Systems Induce Cell Spheroid Formation. *J. Vis. Exp.* (137), e57826, doi:10.3791/57826 (2018).

Abstract

The cellular, biochemical, and biophysical heterogeneity of the native tumor microenvironment is not recapitulated by growing immortalized cancer cell lines using conventional two-dimensional (2D) cell culture. These challenges can be overcome by using bioprinting techniques to build heterogeneous three-dimensional (3D) tumor models whereby different types of cells are embedded. Alginate and gelatin are two of the most common biomaterials employed in bioprinting due to their biocompatibility, biomimicry, and mechanical properties. By combining the two polymers, we achieved a bioprintable composite hydrogel with similarities to the microscopic architecture of a native tumor stroma. We studied the printability of the composite hydrogel *via* rheology and obtained the optimal printing window. Breast cancer cells and fibroblasts were embedded in the hydrogels and printed to form a 3D model mimicking the *in vivo* microenvironment. The bioprinted heterogeneous model achieves a high viability for long-term cell culture (> 30 days) and promotes the self-assembly of breast cancer cells into multicellular tumor spheroids (MCTS). We observed the migration and interaction of the cancer-associated fibroblast cells (CAFs) with the MCTS in this model. By using bioprinted cell culture platforms as co-culture systems, it offers a unique tool to study the dependence of tumorigenesis on the stroma composition. This technique features a high-throughput, low cost, and high reproducibility, and it can also provide an alternative model to conventional cell monolayer cultures and animal tumor models to study cancer biology.

Video Link

The video component of this article can be found at <https://www.jove.com/video/57826/>

Introduction

Although 2D cell culture is widely used in cancer research, limitations exist as the cells are grown in a monolayer format with a uniform concentration of nutrients and oxygen. These cultures lack important cell-cell and cell-matrix interactions present in the native tumor microenvironment (TME). Consequently, these models poorly recapitulate physiological conditions, resulting in aberrant cell behaviors, including unnatural morphologies, irregular receptor organization, membrane polarization, and abnormal gene expression, among other conditions^{1,2,3,4}. On the other hand, 3D cell culture, where cells are expanded in a volumetric space as aggregates, spheroids, or organoids, offers an alternative technique to create more accurate *in vitro* environments to study fundamental cell biology and physiology. 3D cell culture models can also encourage cell-ECM interactions that are critical physiological characteristics of the native TME *in vitro*^{1,4,5}. The emerging 3D bioprinting technology provides possibilities to build models that mimic the heterogeneous TME.

3D bioprinting is derived from rapid prototyping and enables the fabrication of 3D microstructures that are capable of mimicking some of the complexities of living tissue samples^{6,7}. The current bioprinting methods include inkjet, extrusion, and laser-assisted printing⁸. Among them, the extrusion method allows the heterogeneity to be controlled within the printed matrices by precisely positioning distinct types of materials at different initial locations. Therefore, it is the best approach to fabricate heterogeneous *in vitro* models involving multiple types of cells or matrices. Extrusion bioprinting has been successfully used to build auricular shaped scaffolds⁹, vascular structures^{10,11,12}, and skin tissues¹³, resulting in high printing fidelity and cell viability. The technology also features versatile material selections, the ability to deposit materials with cells embedded with a known density, and high reproducibility^{14,15,16,17}. Natural and synthetic hydrogels are frequently used as bioinks for 3D bioprinting due to their biocompatibility, bioactivity, and their hydrophilic networks that can be engineered to structurally resemble the ECM^{7,18,19,20,21,22,23}. Hydrogels are also advantageous since they can include adhesive sites for cells, structural elements, permeability for nutrients and gases, and the appropriate mechanical properties to encourage cell development²⁴. For instance, collagen hydrogels offer integrin

anchorage sites that cells can use to attach to the matrix. Gelatin, denatured collagen, retains similar cell adhesion sites. In contrast, alginate is bioinert but provides mechanical integrity by forming crosslinks with divalent ions^{25,26,27,28}.

In this work, we developed a composite hydrogel as a bioink, comprised of alginate and gelatin, with similarities to the microscopic architecture of a native tumor stroma. Breast cancer cells and fibroblasts were embedded in the hydrogels and printed via an extrusion-based bioprinter to create a 3D model that mimics the *in vivo* microenvironment. The engineered 3D environment allows cancer cells to form multicellular tumor spheroids (MCTS) with a high viability for long periods of cell culture (> 30 days). This protocol demonstrates the methodologies of synthesizing composite hydrogels, characterizing the materials' microstructure and printability, bioprinting cellular heterogeneous models, and observing the formation of MCTS. These methodologies can be applied to other bioinks in extrusion bioprinting as well as to different designs of heterogeneous tissue models with potential applications in drug screening, cell migration assays, and studies that focus on fundamental cell physiological functions.

Protocol

1. Preparation of the Materials, Hydrogel, and Cell Culture Materials

1. Material and solution preparation

1. Wash and dry 250 mL and 100 mL glass beakers, magnetic stirrers, spatulas, 10 mL cartridges, 25 G cylindrical nozzles (with a length of 0.5 in and an inner diameter of 250 μ m). Sterilize the materials by autoclaving them at 121 °C/15 min/1 atm. Keep the materials under sterile conditions until use.

Note: Refer to the **Table of Materials** for vendor information.

2. Weigh 3 g of alginate (3% w/v) and 7 g of gelatin (7% w/v) (denoted as A3G7 hereafter).
3. Sterilize the following items under UV light for at least 4 h: alginate and gelatin powders, paraffin film, aluminum foil pieces of 5 cm², and 1 mL and 5 mL syringes. Sterilize the end caps, tip caps, and pistons by immersing them in 70% ethanol for at least 4 h and wash them 2x with sterilized ultra-pure water.

Note: Refer to the **Table of Materials** for vendor information.

4. Dissolve 4 g of agarose with ultra-pure water and sterilize it by autoclaving.
Note: The agarose is completely dissolved after the autoclaving process.
5. Prepare a 100 mM solution of anhydrous calcium chloride (CaCl₂) in sterilized ultra-pure water and a sterile filter (with a pore size of 0.22 μ m) prior to use.
6. For agarose-coated 6-well plates, melt the sterile agarose in a microwave to obtain a liquid solution; then, under a Biosafety Cabinet (BSC) and using a 1 mL micropipette, add 2 mL per well and mix it gently to create a uniform layer in the bottom of the well. Leave it to cool down and seal the well with paraffin film. Keep it at room temperature (RT) until use.

2. Preparation of the A3G7 hydrogel precursor

1. Mix 3 g of alginate and 7 g of gelatin powders into a 250 mL beaker within a BSC. Add a magnetic stirrer and 100 mL of DPBS. Seal the beaker with sterile paraffin film and aluminum foil (5 cm²) to avoid contamination.
2. Dissolve the powders under a constant agitation in a magnetic/hot plate with 600 rpm at 60 °C for 1 h and at RT for an extra 2 h.
3. Heat the material at 37 °C until the gel undergoes a phase transition to the liquid state (for 100 mL of stock gel solution, this takes approximately 45 min). Transfer the solution into sterile 50 mL conical centrifuge tubes, seal them, and centrifuge the tubes at 834 x g for 5 min to eliminate any gas bubbles from the material.
4. Aspirate the hydrogel precursor into 10 mL syringes. Seal the syringes with caps and paraffin film. Store them at 4 °C until use.

3. Cell culture

Note: The steps in this section must be performed under sterile conditions.

1. Prepare the basal DMEM medium as follows (for 1 L): in a BSC, mix 100 mL of fetal bovine serum (FBS) plus 10 mL of an antibiotic/antimycotic solution (a 100x stabilized solution) into a fresh sterile container. Add DMEM medium to adjust the mixture up to 1,000 mL. Seal the container and keep it at 4 °C.
2. In a previously warmed water bath (37 °C), defrost 1 vial of MDA-MB-231-GFP (human breast cancer cell line GFP-labeled, nuclear localization) and 1 vial of IMR-90-mCherry (cancer-associated fibroblast cell lines mCherry-labeled, with cytoplasmic localization) cells from the liquid nitrogen storage by moving them gently into the water. Both cell lines, and the plasmids for GFP and mCherry labeling, are commercially available.
3. Transfer 160 μ L/well of cell solution (3 x 10⁶ cell/mL) into a 6-well plate and add 5 mL of warmed (37 °C) basal DMEM medium. Incubate the plate at 37 °C/5% CO₂ for 24 - 48 h until the cells reach 80% confluence.
4. After the cells reach confluence, discard the medium and rinse the cells twice with DPBS; incubate the cells with 500 μ L of trypsin-EDTA solution/well (0.25%, 1x, previously warmed at 37 °C) at 37 °C for 6 min. Then, inactivate the trypsin by adding 500 μ L of FBS, recover the cell solution and transfer it to T-75 flasks. Incubate them again at 37 °C/5% CO₂ until the cells reach 80% confluence.
Note: The volume of trypsin-EDTA solution can vary depending on the cell-growth vessel.
5. Repeat the previous step to work with cells on passage 3 - 4 as that is when cells have more metabolic activity and stability.
6. Count the cells using a trypan blue assay (0.4%) to determine the initial concentration of cells to be mixed with the hydrogel.

2. Measurements of Rheological Properties of Hydrogels

1. Prepare the alginate/gelatin hydrogel precursor as described in step 1.2.
Note: Sterile conditions are not required for samples generated for mechanical testing and analysis. All rheological tests are performed in triplicate.
2. Take a syringe of the hydrogel precursor and warm it up in a 37 °C water bath for 1 h.

3. Turn on the rheometer and initialize the system according to the following steps.
 1. Turn on the air compressor connected to the rheometer and let the air compressor run for 30 min. Switch on the temperature control box for the rheometer, switch on the rheometer itself, and switch on the computer connected to the rheometer.
 2. Open the rheometer software, click **Initialize** on the control panel, and let the initialization process finish. Set the platform temperature to 37 °C on the control panel.
 3. Click the **Measuring set** tab and navigate to the **Start service function**, select **Adjust driver inertia** in the drop-down menu, and click **Start adjustment** in the pop-up window.
 4. Mount a parallel measuring tool in the rheometer. All the experiments performed here use a 25 mm diameter plate with a 1 mm gap between the plates.
 5. Click **Set zero-gap** on the control panel and wait for the procedure to finish. Pay attention to the normal force during this process. Note: After this procedure, the normal force should be 0.
 6. Click the **Measuring set** tab and navigate to the **Start service function**, select **Adjust upper measuring system inertia**, and click **Start adjustment** in the pop-up window. Once done, click the triangle button on the control panel to allow the measuring tool to move up.
4. Conduct an amplitude sweep.
 1. Click **Start**, then click **Insert** in the top menu, select **Wait** from the drop-down menu. Pull up the setup window and set the waiting time to 2 h. Note: This will add a waiting step before the tests.
 2. Click **Start**, then click the **Insert** button again, and from the drop-down menu, select **Device**. Pull up the setup window, choose **Temperature**, and set it to be 25 °C. Uncheck the box of **Wait until value is reached**.
 3. Click the step **Measurement**, then click the variable **Oscillation strain**, pull up the setup window, set **Profile** to be **Ramp logarithm**, and change the value to 0.001% and 100% as the initial strain and final strain, respectively. Set the frequency at 0.01 Hz.
 4. Click the **Add** button to add the **Temperature** variable. Click the variable **Temperature** and set it to be 25°C. In the pull-up window, expand **Calculator**, set **Point density** to 10 points/decade.
 5. Take the syringe out of the water bath and extrude approximately 0.5 mL of the precursor onto the rheometer platform.
 6. Click the downwards triangle button on the control panel. Wait for the measuring tool to move down to the trimming position.
 7. Use a spatula to trim any excess precursors that escaped at the edge of the measuring tool and discard the superfluous material.
 8. Pipette mineral oil onto the edge of the measuring tool and wait until the oil fully seals the boundary.
 9. Click **Continue** on the control panel. Then click the **Start** button (green triangle), followed by clicking **Continue** button at the bottom screen.
 10. When the testing is done, release the measuring tool, and then click the upwards triangle button on the control panel. Remove the measuring tool and clean it with 70% ethanol. Clean the platform with 70% ethanol.
 11. In the current project, click the step **Measurement** and pull up the setup window. Now, set the frequency to 100 Hz. Keep all other parameters unchanged.
 12. Repeat steps 2.4.5 - 2.4.10.
 13. Click **Diagram**. Observe the curve of G' , G'' versus the oscillation strain. Find the deflection points of G' for both frequencies (0.01 Hz and 100 Hz). Find the corresponding oscillation strains for both deflection points.
 14. Choose the smaller oscillation strain and use 1/10 of this strain for all oscillation tests conducted afterward. Note: The onset of G' deflection is considered the ultimate linear elastic strain (ULES) that should not be exceeded in follow-up tests. The ratio 1/10 is usually used in engineering for safety reasons. This calculated strain is denoted as g_c .
 15. After the test is done, click **Table**, copy all data, and paste it into a text file.
5. Conduct a temperature sweep.
 1. Click **My apps** and select the template **Temperature ramp, oscillatory shear: Gelation**.
 2. Name the project.
 3. Click the step **Measurement** in the workflow. Then click the variable **Temperature**, pull up the setup window, and set the initial and final temperature to be 37 °C and 25 °C, respectively.
 4. In the pull-up window, set oscillation strain to 0.1%, oscillation frequency to 1Hz. Then set the number of data points to be 61. Set the data collection frequency to 1 point/min. Click **Calculator** and set **Point density** to 0.2 °C/point. Note: This will allow the temperature to change at a rate of 0.2 °C/min.
 5. Load the sample on the rheometer platform and perform the test by following steps 2.4.5 - 2.4.10.
 6. Click **Diagram**, observe the G' , G'' versus the temperature. Find the crossover point of G' and G'' . Find the temperature at the crossover point. Note: This is the sol/gel transition temperature of the hydrogel precursor.
 7. Repeat step 2.4.15.
6. Conduct an isothermal time sweep.
 1. Click **My apps** and find and click the template **Isothermal time-temperature test**. Click the step **Measurement** in the workflow, and then click the variable **Oscillation strain**, pull up the setup window, set the oscillation strain to 0.1%, and set the oscillation frequency to 1 Hz. In the pull-up window, set the number of data points to 120. Set the data collection frequency to 1 point/min. Note: The value of this strain is based on the results from the amplitude sweep.
 2. Click **Add** button to add the **Temperature** variable. Click variable **Temperature** in the middle window and set it to 25 °C.
 1. Right click the step **Device move to measuring point** in the workflow, click **delete**. Then click the step **Device set value**, uncheck the box **Wait until value is reached**, and set value to 25 °C. Click **Picture, title, buttons** at the bottom screen, uncheck the box **Continue**. Then click the step **Start**, name the project and save it.
 3. Load the sample onto the rheometer platform and start the test by following steps 2.4.5 - 2.4.10.
 4. Observe the G' , G'' versus the time. Find the crossover point of G' and G'' . Find the time at the crossover point. After the test is done, click **Table**, copy all data, and paste it into a text file.

Note: This is the sol/gel transition time of the hydrogel precursor at 25 °C.

7. Measure the yield strength at various gelling times.
 1. Click **My apps** and find and click the template **Yield and flow stress, Gel-like**. Name the project. Click the step **Start** in the workflow. Click **Insert** in the top menu and, in the drop-down menu, select **Wait**. Pull up the setup window and set the waiting time to be 20 min. Note: This will add a waiting step before the tests.
 2. Click **Start**, then click **Insert** again and, in the drop-down menu, select **Device**. Pull up the setup window, chose **Temperature**, and set it to 25 °C. Uncheck the box **Wait until value is reached**.
 3. Click the step **Measurement** in the workflow, select the variable **Shear stress**, pull up the setup window, and set the initial and final shear stress to 0 and 10,000 Pa, respectively. Click **Calculator**, set the **Point density** to 0.2 point/Pa. In the **Data points** tab on the left, set 1 point/ second. Note: this will result in a stress ramping rate of 5 Pa/s.
 4. Click the **Event control** tab at the bottom of the pull-up window and set the stop criterion: stop the measurement if the shear rate > 100 s⁻¹. Note: This will automatically stop the measurement if the material is yielded.
 5. Load the sample onto the rheometer platform and start the test by following steps 2.4.5 - 2.4.10.
 6. Click **Diagram**. Observe the strain-stress curve. Find the deflection point of the strain and its corresponding stress. Repeat steps 2.7.2 - 2.7.6, but change the waiting time to 30, 40, and 50 min for each replicate; this will result in the yield strength at different gelling times. Note: This stress is regarded as the apparent yield strength. Note: software clicks can differ by rheometer models and software versions. We recommend readers to take reference of the testing parameters we provide, while refer to the manual of specific rheometer/software in practical use.

3. Scaffold Design, Cell-laden Hydrogel, and 3D Printing Models

1. Scaffold design

1. Draw a propeller-like model on paper. Note: The propeller-like model is designed based on the following considerations: (a) it simulates the *in vivo* scenario where cancer cells are surrounded by CAFs; (b) it minimizes the concentration of stress *via* the use of circular geometries; (c) it is flexible so that more sectors can be added into the model in the future without changing the existing geometries; and (d) it is flat in its vertical scale to facilitate nutrient diffusion.
2. Let the center of the propeller be the origin and use the symbols R_0 , R_1 , and R_2 to represent the maximal radius of the inner circle, middle sectors, and outer sectors, respectively. Use the symbols m and n to represent the number of internal arcs and spokes inside the sector area, respectively.
3. Calculate the coordinates of each node on the propeller-like model and write them in the symbolic expressions of R_0 , R_1 , R_2 , m , and n .
4. Start a program script, set R_0 , R_1 , R_2 , m , and n as variables, and input the symbolic expression of each key node. Note: Refer to the **Table of Materials** for any software information.
5. Arrange a path that connects the nodes and assign a cartridge for the inner circle, the middle sectors, and the outer sectors. Set the layer thickness to be 150 μm and the number of layers to be 4.
6. Let the program output a text file in G-code format that is recognizable by the bioprinter.
7. Set $R_0 = 3.85$, $R_1 = 6.85$, $R_2 = 8.65$, $m = 2$, and $n = 5$. Run the script and retrieve the generated G-code file. Copy and paste the file to the bioprinter's dedicated G-code folder.
8. Turn on the bioprinter and its control software. Initialize the printer. Open the G-code script just created and set all pressures to zero. Return to the control software, click the tab **Scaffolder generator**, and then click the **Run** button at the right bottom corner. Observe the moving path of the printer. Note: This will test the precision of the generated G-code. Refer to the **Table of Materials** for information related to the bioprinter.
9. This step is optional. Build a demonstrative 3D model based on the parameters above *via* computer-aided design (CAD) software. Note: Refer to the **Table of Materials** for the vendor software information.

2. Make a cell-laden A3G7 hydrogel precursor

Note: The steps in this section must be performed under sterile conditions. Keep the bioprinter inside a BSC.

1. Sterilize the bioprinter by spraying 70% ethanol thoroughly and exposing it to UV light overnight.
2. Take out a syringe of the hydrogel precursor (at 4 °C) and warm it in a water bath at 37 °C for 1 h.
3. Take the T-flask with cells (see step 1.3) from the CO₂ incubator and place it inside a BSC. Discard the culture medium and rinse the cells with DPBS twice. Add a warmed trypsin-EDTA solution (3.0 mL) and incubate the cells at 37 °C for 6 min. Inactivate the trypsin with a same volume of FBS. Count the cells using trypan blue assay.
4. Take the syringe of the hydrogel precursor from the water bath, clean it, and sterilize it with 70% ethanol. Put the syringe into the BSC.
5. Extrude approximately 3 mL of hydrogel precursor into a 10 mL printing cartridge. Mix the precursor with MDA-MB-231-GFP cells at 1 x 10⁶ cells/mL by slowly pipetting it, avoiding the production of bubbles. Cover the cartridge with the sterile end and top caps and seal it with paraffin film. Centrifuge it at 834 x g for 1 min to eliminate any gas bubbles produced.
6. Repeat steps 3.2.3 - 3.2.5 for the IMR-90-mCherry cell-laden precursor and the cell-free precursor.
7. Sterilize all 3 cartridges with 70% ethanol and then load them into the chambers of the bioprinter. In the printer's control software, set the cartridge temperature to 25 °C. Wait 35 min to allow the precursor to reach printable conditions. Note: This time does not affect the viability of the cells embedded in the hydrogel.

3. 3D printing models

1. In the printer's control software, expand the **Tool head** tab in the printer's control software, click on 1 cartridge at the graphic interface at the left side, and then click the **Measure short** button to measure the position of the nozzle tip. Repeat this for the other 2 cartridges.

2. Place a clear polystyrene microplate, open the G-code file, and change the pressure to 200 kPa for all cartridges. Return to the control software, click the tab **Scaffolder generator**, select a point to start printing, and then click the **Run** button at the right bottom corner. Repeat this step to get 3 more replicates.
3. After printing all replicates of the propeller models, add a 100 mM CaCl₂ solution to cross-link the models for 1 min and rinse it 2x with DPBS to remove the excess of Ca⁺⁺ ions.
4. Carefully transfer the models onto an agarose-coated 6-well plate using a spatula. Add 5 mL of DMEM media to each well. Incubate the plates in an incubator at 37 °C and 5% CO₂.
Note: make sure the models are floating in the wells.
5. Replace the cell culture medium with fresh medium every 3 days, culture it for 30 days in total.

4. Viability and Spheroid Formation Experiments on the Hydrogel Disks.

1. Hydrogel disk preparation

1. Repeat steps 3.2.1 - 3.2.6.
Note: It is possible to substitute the cartridge with a small sterile container.
2. Use a sterile graduated 1 mL syringe and cut the nozzle to create a large hole in the syringe (the hole has the same diameter as the rest of the syringe tube). Clean it with 70% ethanol and leave it until it is dry.
Note: Do this in a sterile BSC.
3. Use a well-plate lid, add 100 mM CaCl₂ until the surface is covered; then, take the cell-laden hydrogel to fill the syringe; extrude 100 µL using the hanging drop method. Leave the hydrogel for 1 min and rinse it with excessive DPBS. Transfer the hydrogel disks onto an agarose-coated 6-well plate, add 5 mL of basal DMEM, and incubate them at 37 °C and 5% CO₂ for up to 30 days. Refresh the medium every 3 days.

2. Cell and spheroid viability

1. Use an MTS assay to determine the cell viability. Wash each disk with DPBS and cut it into 4 parts with a fine sterile blade. Collect the parts of the whole disk and transfer them to a 96-well plate. Then, add 100 µL of DMEM plus 20 µL of MTS reagent to each well and incubate the mixture at 37 °C for 2 h.
2. After the MTS reaction, recover the supernatant and transfer it to a clean 96-well plate. Measure the absorbance of the samples at 490 nm.

3. Spheroid formation

1. Take out the incubated propeller or disk model from the incubator at days 0, 7, 15, 21, and 30 of the culture and transfer them to a clean 6-well plate.
2. Use a confocal spinning disk inverted microscope to visualize the spheroids and acquire the images using multiple positions and z-stacks. Image each propeller, or disk model, along its horizontal diameter from left to right with a 500 µm gap and acquire a z-stack from the bottom to the top focal plane at each horizontal position.
Note: Refer to the **Table of Materials** for the vendor information.
3. Reconstruct the image using a maximum stack arithmetic tool, provided by the program ImageJ, to create the 2D images used for a spheroid analysis.

5. Scanning Electron Microscopy (SEM)

1. Prepare the alginate/gelatin hydrogel as described in step 1.2.
Note: Sterile conditions are not required.
CAUTION: Liquid nitrogen and paraformaldehyde are dangerous and must be handled with care.
2. Put 1 mL of hydrogel into a mortar, add liquid nitrogen, and grind it using a pestle. Continue adding liquid nitrogen to avoid the hydrogel from defrosting. Transfer the powder into a 1.5 mL centrifuge tube, seal it, and store it at -80 °C for 2 h. Freeze-dry the sample for 24 h.
3. For spheroid imaging, wash the hydrogel gently with DPBS 2x, fix the cells by immersion in 4% paraformaldehyde for 30 min at 37 °C, and then rinse them with DPBS and freeze them with liquid nitrogen. Finally, freeze-dry the sample for 24 h.
4. Analyze the hydrogel/spheroid structure and morphology with a scanning electron microscope (SEM) at 25.0 kV, under 70 Pa (chamber pressure) with a magnification of 40X up to 5,000X.

Representative Results

The temperature sweep shows a distinct difference of the A3G7 precursor at 25 °C and 37 °C. The precursor is liquid at 37 °C and has a complex viscosity of 1938.1 ± 84.0 mPa s, which is validated by a greater G'' over G' . As the temperature decreases, the precursor undergoes physical gelation due to the spontaneous physical entanglement of the gelatin molecules into a tri-helix formation^{29,30}. Both the G' and the G'' increase and converge at 30.6 °C, indicating a sol-gel transition. The moduli continue to increase, with decreased temperature, reaching 468.5 ± 34.2 Pa of G' and 140.7 ± 9.3 Pa of G'' at 25 °C (**Figure 1a**). Based on the results of the temperature sweep, we chose 25 °C as the printing temperature. The gelation kinetics experiment simulates the temperature change that occurs during the sample preparation and handling (*i.e.*, removing the sample from the 37 °C water bath and placing it into the 25 °C bioprinter chamber). G' , G'' , and $|\eta^*|$ increase with time at the lowered temperature, and the sol-gel transition happens at ~ 17 min at 25 °C, when $G' \approx G'' \approx 64.3$ Pa and the loss factor equals 1 (**Figure 1b** and **1c**). The precursor continues to stiffen and reaches a printing window after 50 - 90 min of gelation. Within this printing window, the precursor can be smoothly extruded using a G25 cylindrical nozzle with a pressure of 200 kPa. The existence of yield stress implies a solid-like behavior of the material and raises the structural integrity after the extrusion to withstand its own weight³¹. The stress ramp recognizes the yield stress at different times of the gelation. Results show that the yield stress increases with the increasing gelation time. At 50 min of gelation, the yield stress reaches 325.9 Pa, assuring that the model is stable after the extrusion.

The printed propeller model is shown in **Figure 2a**. Confocal microscopy confirms the initial extrusion locations of both the MDA-MB-231-GFP and the IMR-90-mCherry cells (**Figure 2b**). The MDA-MB-231-GFP cells begin to develop spheroids 15 days into the culture period, followed by increased size and numbers of spheroids until day 30 (**Figure 2c - 2f**). Some of the IMR-90-mCherry cells also form agglomerations (**Figure 2g - 2j**). Noticeably, after 30 days of culture, IMR-90-mCherry cells are observed in the region initially occupied by the MDA-MB-231-GFP cells (**Figure 2f**), implying possible migration events in the model. Likewise, migrated MDA-MB-231-GFP cells can also be observed in the IMR-90-mCherry dominated region on day 30 (**Figure 2j**).

The disk model is shown in **Figure 3a**. Confocal microscopy confirms the homogeneous cell distribution within the disk (**Figure 3b**). The MDA-MB-231-GFP cells behave similarly in the disk model as they did when printed as a propeller model. Representative images are displayed in **Figure 3c - 3f**. SEM imaging reveals an MDA-MB-231-GFP spheroid-laden hydrogel after 21 days of culture (**Figure 4a**). The generation, and presence, of the spheroid is validated by comparing the SEM images with cell-free hydrogels (**Figure 4b**).

The cell viability of both cell types is demonstrated in **Figure 4c**. MDA-MB-231-GFP cells express a higher cell viability compared to IMR-90-mCherry cells. Interestingly, the MDA-MB-231-GFP cells exhibit an increased trend of viability before day 15, with a tripling of the number of viable cells compared to day 0. This is followed by a decrease on day 21, before recovering again on day 30. In contrast, the IMR-90-mCherry cells have minimal fluctuations in viability during the entirety of the culture period. The decreasing values in viability of the MDA-MB-231-GFP cells at day 21 correspond to a large MTCSs formation, which has developed necrotic cores.

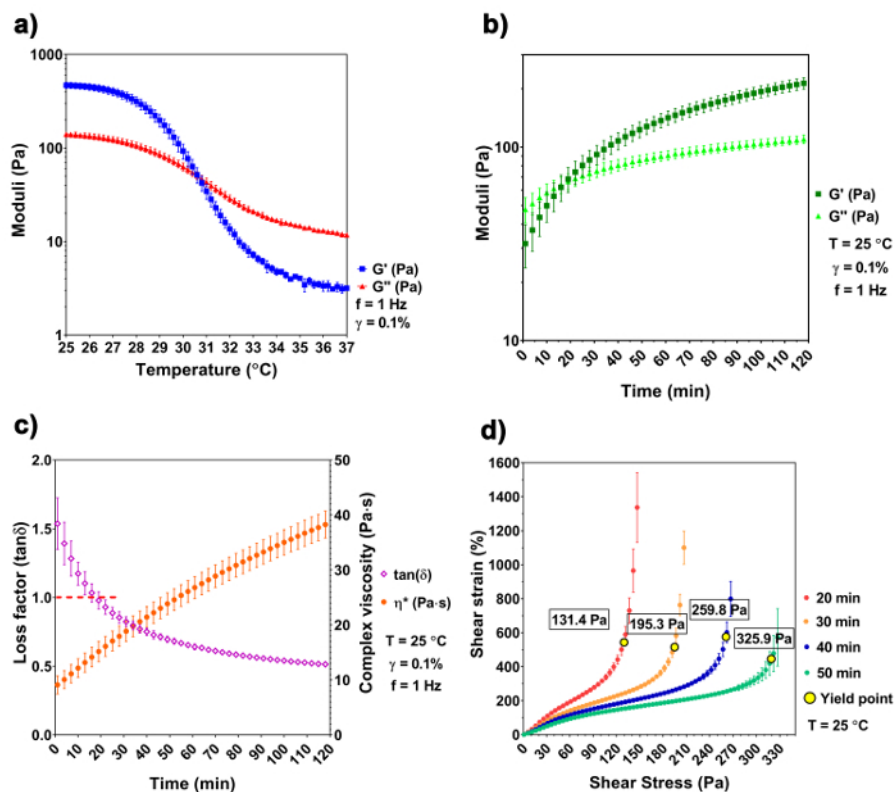


Figure 1: Rheological characterization of the hydrogel precursor. (a) A temperature sweep shows the sol-gel transition at 30.6 °C. (b-c) The gelation kinetics of the A3G7 precursor shows an increase of G' , G'' , and $|\eta^*|$ at time of gelation, and the sol-gel transition happens at approximately 17 min at 25 °C. (d) This panel shows the yield stress of the precursor *versus* the time of gelation. An increase of yield stress is observed with a longer gelling time. The results are shown in mean \pm SD, $n \geq 3$. [Please click here to view a larger version of this figure.](#)

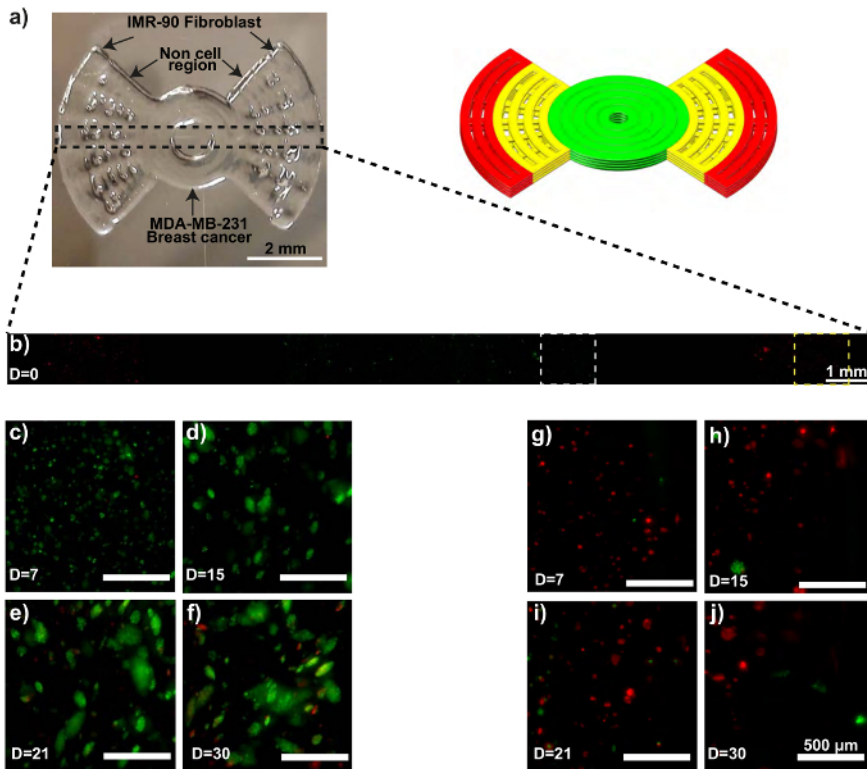


Figure 2: MCTS formation within a 3D bioprinted *in vitro* model consisting of IMR-90-mCherry myofibroblast and MDA-MB-231-GFP breast cancer cells. (a) These photographs show the bioprinted *in vitro* sample (left) and the CAD model (right). (b) This representative confocal time-lapse image shows the MDA-MB-231-GFP (green) and IMR-90-mCherry (red) cells bioprinted within the model. (c - f) These zoom-ins show the MDA-MB-231-GFP cell regions (white dotted boxes). (g - j) These zoom-ins show the IMR-90-mCherry cell regions (yellow dotted boxes). The scale bars are 2 mm in panel 2a, 1 mm in panel 2b, and 500 μm in panels 2c - 2j for selected areas, and the magnification is 10X. Capital "D" in the images means "days of culture". [Please click here to view a larger version of this figure.](#)

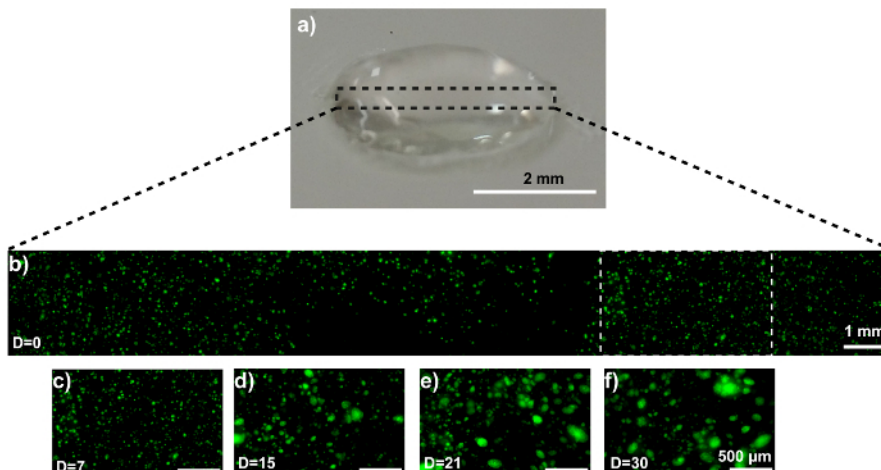


Figure 3: MCTS formation within a 3D MDA-MB-231-GFP-laden hydrogel disk. (a) This photograph shows a hydrogel disk. (b) This representative confocal image shows MDA-MB-231-GFP cells embedded in the composite. (c-f) These zoom-ins show the MDA-MB-231-GFP cell region (white dotted box in panel 3b) at (c) 0, (d) 7, (e) 15, and (f) 21 days of culture. The scale bars are 2 mm in panel 3a, 1 mm in panel 3b, and 500 μm in panels 3c - 3f for selected areas, and the magnification is 10X. Capital "D" in the images means "days of culture". [Please click here to view a larger version of this figure.](#)

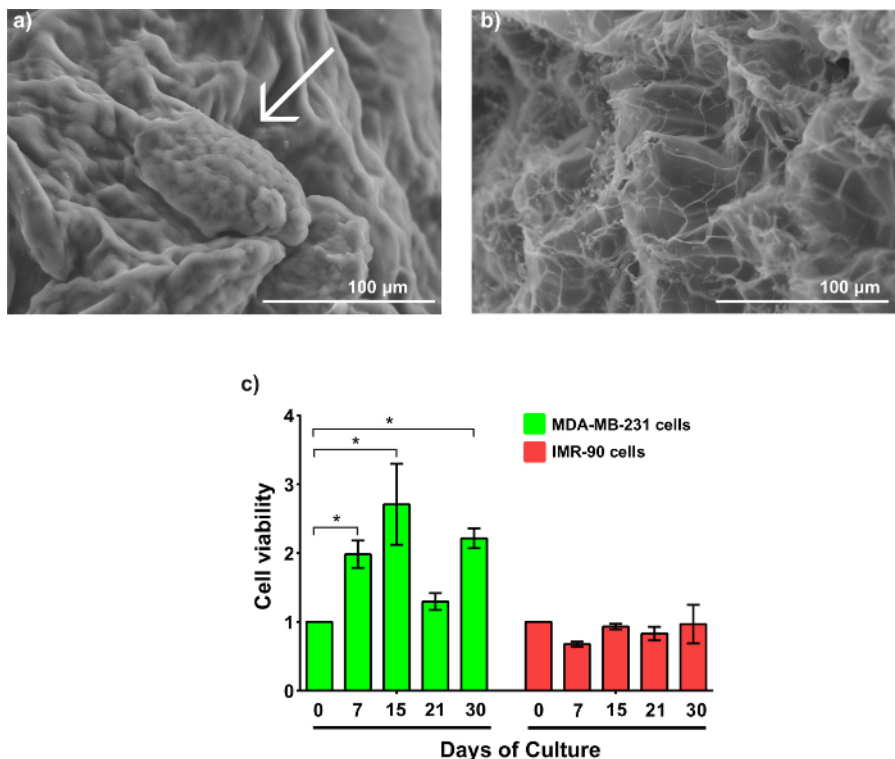


Figure 4: Morphology and cell viability of MTCSSs. (a) This SEM image shows an MDA-MB-231-GFP MTCSS within the gel after 21 days of culture, showing small MTCSS (arrow-pointed). (b) This SEM image shows an alginate/gelatin hydrogel without cells. The magnification is 350X. (c) This panel shows the cell viability of MDA-MB-231-GFP and IMR-90-mCherry during 30 days of culture within the hydrogel. The results were analyzed as the mean \pm SD and statistically analyzed using a two-way ANOVA and a Bonferroni's post-test. p (*) < 0.05 , $n \geq 3$. The data was normalized to the cell density used to create the samples on day 0. [Please click here to view a larger version of this figure.](#)

Discussion

Cell-laden structures can be compromised if contamination (biological or chemical) occurs at any point in the process. Usually, biological contamination is seen after two or three days of culture as a color change in the culture media or the bioprinted structure. Therefore, the sterilization (physical and chemical disinfection) is a key step for all the cell-related processes. Noteworthy, autoclaving gelatin changes its gelling properties, which made it gel slower in the trials we conducted. Therefore, we sterilized the alginate and gelatin power via UV exposure. Due to the very limited penetration capability of UV light, a very thin layer (< 0.5 mm) should be used. The concentration of alginate and gelatin can be arbitrarily changed to tune the mechanical and biological properties³². In the present work, we chose A3G7, because it provides desirable printability during its printing window, and the crosslinked hydrogel provides a high stability through the 30-day experiment. Heating to 60 °C while dissolving powder into DPBS helps to enhance the liquefaction of gelatin, which eases the stirring. A lower temperature can also be used; however, a longer stirring time will then be required.

The rheological temperature sweep gives a sol-gel point at 30.6 °C, which is compatible with other publications³³. Theoretically, any temperature higher than 30.6 °C can liquefy the precursor. We chose 37 °C to simplify the work, as cell culture medium is pre-warmed in a 37 °C water bath. Based on the gelation kinetics (before the precursor gels), there is approximately 17 min for cell mixing; after this time, mixing the cells and the hydrogel precursor is difficult due to the increased viscosity and moduli, causing a non-homogeneous cell-laden bioink. Therefore, we suggest handling the cell-mixing work within the first 10 min of gelling. The yield stress is not considered to be a material attribute that affects printability until recently³⁴, regardless, it has been extensively recognized by polymer scientists as a marker of pasty/granular fluid^{31,35,36,37}. The existence of yield stress helps to build up a structural integrity to withstand its own weight. A high yield stress can also require an increased startup pressure in extrusion; thus, this may result in damage to the cells due to excessive shear stress³². The model fidelity can be compromised if the extrusion process occurs outside of the optimal printing window. Common indicators of this problem are shown in the final bioprinted structure: it will either be too rough or too liquid at the edges. The A3G7 precursor exhibits an optimal printing window during 50 - 90 min of gelling that satisfies both the structural stability and the cell survival and can be used as the medium to build heterogeneous tumor models¹⁴.

The total height of the propeller model is 600 μ m as it is generated from four layered 150 μ m filaments. This design allows nutrient and gas exchange as cells are at most 300 μ m from the surface contacting the media during the incubation. Higher models are achievable in fabrication but are bottlenecked by the limited diffusion distance of the nutrients in the hydrogel³⁸, which can result in a low cell survival in the core region.

Different strategies have been developed to form MCTS *in vitro*, such as hanging drop, microfluidic chip, assembly, and bioprinting³⁹. However, some of these methodologies can alter the cell physiology and biochemistry, generating different cell behaviors that occur in normal tumor tissue. For instance, the hanging drop method forces single cells to stay as cell aggregates through physical confinement⁴⁰. Also, the chemical induction to form MCTS by a peptide addition can alter the biochemistry of the spheroids⁴¹. The hydrogel composite described here allows an MCTS

formation by creating a biomimetic environment without external stressors. Starting out as single well-dispersed cells, after 7 days of cultures, cells reorganize as small MCTS (more than 6 cells per spheroid), increasing their size and quantity during 30 days of culture.

In the results of this research, we found that MDA-MB-231-GFP spheroids decrease the cell viability at day 21, correlating this phenomenon with the formation of large spheroids. A solid tumor is comprised of three different layers, whereby the external layer presents a high proliferation rate compared to the middle layer and the internal necrotic or senescent core of the spheroid¹⁸. This could explain the viability decrease in the results.

This limitations of this protocol are (1) bioink dynamics and (2) cell type compatibility. Bioink dynamics refers to the varying material properties during the gelation process, resulting in an optimal printing window beyond which the printed structure is defective. Cell type compatibility refers to the incapacity of certain cell types (cell line or primary culture) to exhibit a native *in vivo* behavior.

The A3G7 hydrogel achieves a high stability and cell viability. 3D bioprinting can be used to build 3D heterogeneous disease models with high-throughput, low cost, and high reproducibility as a more realistic alternative to traditional cell culture and small animal tumor models.

Disclosures

The authors have nothing to disclose.

Acknowledgements

Tao Jiang thanks the China Scholarship Council (201403170354) and McGill Engineering Doctoral Award (90025) for their scholarship funding. Jose G. Munguia-Lopez thanks CONACYT (250279, 290936 and 291168) and FRQNT (258421) for their scholarship funding. Salvador Flores-Torres thanks CONACYT for their scholarship funding (751540). Joseph M. Kinsella thanks the National Science and Engineering Research Council, the Canadian Foundation for Innovation, the Townshend-Lamarre Family Foundation, and McGill University for their funding. We would like to thank Allen Ehrlicher for allowing us to use his rheometer, Dan Nicolau for allowing us to use his confocal microscope, and Morag Park for granting us access to fluorescently labeled cell lines.

References

- Cui, X., Hartanto, Y., Zhang, H. Advances in multicellular spheroids formation. *Journal of the Royal Society Interface*. **14** (127), (2017).
- Yip, D., Cho, C. H. A multicellular 3D heterospheroid model of liver tumor and stromal cells in collagen gel for anti-cancer drug testing. *Biochemical and Biophysical Research Communications*. **433** (3), 327-332 (2013).
- Breslin, S., O'Driscoll, L. The relevance of using 3D cell cultures, in addition to 2D monolayer cultures, when evaluating breast cancer drug sensitivity and resistance. *Oncotarget*. **7** (29), 45745-45756 (2016).
- Yue, X., Lukowski, J. K., Weaver, E. M., Skube, S. B., Hummon, A. B. Quantitative proteomic and phosphoproteomic comparison of 2D and 3D colon cancer cell culture models. *Journal of Proteome Research*. **15** (12), 4265-4276 (2016).
- Priwitaningrum, D. L. *et al.* Tumor stroma-containing 3D spheroid arrays: a tool to study nanoparticle penetration. *Journal of Controlled Release*. **244** (Pt B), 257-268 (2016).
- Hong, S. *et al.* Cellular behavior in micropatterned hydrogels by bioprinting system depended on the cell types and cellular interaction. *Journal of Bioscience and Bioengineering*. **116** (2), 224-230 (2013).
- Dolati, F. *et al.* *In vitro* evaluation of carbon-nanotube-reinforced bioprintable vascular conduits. *Nanotechnology*. **25** (14), 145101 (2014).
- Murphy, S. V., Atala, A. 3D bioprinting of tissues and organs. *Nature Biotechnology*. **32** (8), 773-785 (2014).
- Kang, H. W. *et al.* A 3D bioprinting system to produce human-scale tissue constructs with structural integrity. *Nature Biotechnology*. **34** (3), 312-319 (2016).
- Miller, J. S. *et al.* Rapid casting of patterned vascular networks for perfusable engineered three-dimensional tissues. *Nature Materials*. **11** (9), 768-774 (2012).
- Jia, W. *et al.* Direct 3D bioprinting of perfusable vascular constructs using a blend bioink. *Biomaterials*. **106**, 58-68 (2016).
- Kolesky, D. B., Homan, K. A., Skylar-Scott, M. A., Lewis, J. A. Three-dimensional bioprinting of thick vascularized tissues. *Proceedings of the National Academy of Sciences of the United States of America*. **113** (12), 3179-3184 (2016).
- Lee, V. *et al.* Design and fabrication of human skin by three-dimensional bioprinting. *Tissue Engineering Part C: Methods*. **20** (6), 473-484 (2014).
- Jiang, T. *et al.* Directing the self-assembly of tumour spheroids by bioprinting cellular heterogeneous models within alginate/gelatin hydrogels. *Scientific Reports*. **7** (1), 4575 (2017).
- Knowlton, S., Onal, S., Yu, C. H., Zhao, J. J., Tasoglu, S. Bioprinting for cancer research. *Trends in Biotechnology*. **33** (9), 504-513 (2015).
- Derby, B. Printing and prototyping of tissues and scaffolds. *Science*. **338** (6109), 921-926 (2012).
- Nair, K. *et al.* Characterization of cell viability during bioprinting processes. *Biotechnology Journal*. **4** (8), 1168-1177 (2009).
- Costa, E. C. *et al.* 3D tumor spheroids: an overview on the tools and techniques used for their analysis. *Biotechnology Advances*. **34** (8), 1427-1441 (2016).
- Zhao, Y. *et al.* Three-dimensional printing of Hela cells for cervical tumor model *in vitro*. *Biofabrication*. **6** (3), 035001 (2014).
- Ling, K. *et al.* Bioprinting-based high-throughput fabrication of three-dimensional MCF-7 human breast cancer cellular spheroids. *Engineering*. **1** (2), 269-274 (2015).
- Liang, Y. *et al.* A cell-instructive hydrogel to regulate malignancy of 3D tumor spheroids with matrix rigidity. *Biomaterials*. **32** (35), 9308-9315 (2011).
- Szot, C. S., Buchanan, C. F., Freeman, J. W., Rylander, M. N. 3D *in vitro* bioengineered tumors based on collagen I hydrogels. *Biomaterials*. **32** (31), 7905-7912 (2011).

23. Carey, S. P., Kraning-Rush, C. M., Williams, R. M., Reinhart-King, C. A. Biophysical control of invasive tumor cell behavior by extracellular matrix microarchitecture. *Biomaterials*. **33** (16), 4157-4165 (2012).
24. Hospodiuk, M., Dey, M., Sosnoski, D., Ozbolat, I. T. The bioink: a comprehensive review on bioprintable materials. *Biotechnology Advances*. **35** (2), 217-239 (2017).
25. Caliri, S. R., Burdick, J. A. A practical guide to hydrogels for cell culture. *Nature Methods*. **13** (5), 405-414 (2016).
26. Bhutani, U., Laha, A., Mitra, K., Majumdar, S. Sodium alginate and gelatin hydrogels: viscosity effect on hydrophobic drug release. *Materials Letters*. **164**, 76-79 (2016).
27. Biswal, D. *et al.* Effect of mechanical and electrical behavior of gelatin hydrogels on drug release and cell proliferation. *Journal of the Mechanical Behavior of Biomedical Materials*. **53**, 174-186(2016).
28. Rowley, J. A., Madlambayan, G., Mooney, D. J. Alginate hydrogels as synthetic extracellular matrix materials. *Biomaterials*. **20** (1), 45-53 (1999).
29. Djabourov, M., Leblond, J., Papon, P. Gelation of aqueous gelatin solutions. I. Structural investigation. *Journal de Physique (France)*. **49** (2), 319-332 (1988).
30. Djabourov, M., Leblond, J., Papon, P. Gelation of aqueous gelatin solutions. II. Rheology of the sol-gel transition. *Journal de Physique (France)*. **49** (2), 333-343 (1988).
31. Coussot, P. *Rheometry of Pastes, Suspensions, and Granular Materials: Applications in Industry and Environment*. Wiley-Interscience. Hoboken, NJ (2005).
32. Ouyang, L., Yao, R., Zhao, Y., Sun, W. Effect of bioink properties on printability and cell viability for 3D bioplotting of embryonic stem cells. *Biofabrication*. **8** (3), 035020 (2016).
33. Michon, C., Cuvelier, G., Launay, B. Concentration dependence of the critical viscoelastic properties of gelatin at the gel point. *Rheologica Acta Rheologica Acta: An International Journal of Rheology*. **32** (1), 94-103 (1993).
34. Mouser, V. H. *et al.* Yield stress determines bioprintability of hydrogels based on gelatin-methacryloyl and gellan gum for cartilage bioprinting. *Biofabrication*. **8** (3), 035003 (2016).
35. Benbow, J. J., Oxley, E. W., Bridgwater, J. The extrusion mechanics of pastes-the influence of paste formulation on extrusion parameters. *Chemical Engineering Science*. **42** (9), 2151-2162 (1987).
36. Bingham, E. C. *Fluidity and plasticity*. McGraw-Hill. New York, NY (1922).
37. Horrobin, D. J., Nedderman, R. M. Die entry pressure drops in paste extrusion. *Chemical Engineering Science*. **53** (18), 3215-3225 (1998).
38. Soman, P. *et al.* Cancer cell migration within 3D layer-by-layer microfabricated photocrosslinked PEG scaffolds with tunable stiffness. *Biomaterials*. **33** (29), 7064-7070 (2012).
39. Asghar, W. *et al.* Engineering cancer microenvironments for *in vitro* 3-D tumor models. *Materials Today*. **18** (10), 539-553 (2015).
40. Lin, R. Z., Chang, H. Y. Recent advances in three-dimensional multicellular spheroid culture for biomedical research. *Biotechnology Journal*. **3** (9-10), 1172-1184 (2008).
41. Akasov, R. *et al.* Formation of multicellular tumor spheroids induced by cyclic RGD-peptides and use for anticancer drug testing *in vitro*. *International Journal of Pharmaceutics*. **506** (1-2), 148-157 (2016).